Sensitivity Studies for Space-based Measurement of Atmospheric Total Column Carbon Dioxide Using Reflected Sunlight

Jianping Mao[1] and S. Randolph Kawa[2]

[1]Science System and Applications, Inc., Lanham, MD

[2]Atmospheric Chemistry and Dynamics Branch,

NASA Goddard Space Flight Center, Greenbelt, MD

Abstract

A series of sensitivity studies is carried out to explore the feasibility of space-based global carbon dioxide (CO_2) measurements for global and regional carbon cycle studies. The detection method uses absorption of reflected sunlight in the CO_2 vibration-rotation band at 1.58 μm. The sensitivities of the detected radiances are calculated using the line-by-line model (LBLRTM), implemented with the DISORT (Discrete Ordinates Radiative Transfer) model to include atmospheric scattering in this band. The results indicate that (a) the small (~1%) changes in CO_2 near the Earth's surface are detectable in this CO_2 band provided adequate sensor signal-to-noise ratio and spectral resolution are achievable; (b) the radiance signal or sensitivity to CO_2 change near the surface is not significantly diminished even in the presence of aerosols and/or thin cirrus clouds in the atmosphere; (c) the modification of sunlight path length by scattering of aerosols and cirrus clouds could lead to large systematic errors in the retrieval; therefore, ancillary aerosol/cirrus cloud data are important to reduce retrieval errors; (d) CO_2 retrieval requires good knowledge of the atmospheric temperature profile, e.g. approximately 1K RMS error in layer temperature; (e) the atmospheric path length, over which the CO_2 absorption occurs, must be known in order to correctly interpret horizontal gradients of CO_2 from the total column CO_2

measurement; thus an additional sensor for surface pressure measurement needs to be attached for a complete measurement package.

Introduction

The atmospheric concentration of carbon dioxide (CO_2) has increased by about 1/3 since pre-industrial times, around the year 1750.[1] The increase of CO_2 is caused primarily by fossil fuel combustion, land use change, and biomass burning. Meanwhile the instrumental record of surface temperature over the land and oceans shows that the global mean surface temperature has increased by about half degree in the last century. The linkage between global warming and the increase of atmospheric CO_2 is evident but the details of this linkage are yet to be resolved. On a global mean, CO_2 is the biggest radiative forcing for post-industrial climate change.[1] Although the radiative forcing due to the atmospheric CO_2 concentration change is well understood, the sources and sinks of atmospheric CO_2 are not well known. One of the key issues to assess the future of global warming is to understand the processes controlling the global carbon budget in order to relate anthropogenic emissions of CO_2 quantitatively to atmospheric concentrations.

Currently the ocean and the land together are taking up about half of the anthropogenic CO_2 emissions; the other half remains in the atmosphere. Carbon budget studies have shown that a substantial fraction of the emitted CO_2 cannot be accounted for by the observed atmospheric increase and calculated uptake by oceans.[2] This discrepancy has led to speculation about the nature of the "missing sink" for carbon. The estimated or implied vegetation uptake of CO_2 holds large uncertainties in spatial and temporal distribution and even in the magnitude.[3,4,5] The biggest problem in resolving the carbon budget estimate is the limited data coverage.

The observational foundation of global carbon studies is the NOAA Climate Monitoring and Diagnostics Laboratory (CMDL) carbon cycle greenhouse gases measurement worldwide network.[6] There are total about 56 baseline observatories, fixed sites and tall towers, complimentary with some ship and aircraft measurements. Although the in situ measurements are

highly accurate, their distribution in space and time is necessarily very limited for global process studies. Uncertainty of the global carbon budget estimate based on this network is about 2-3 GtC/yr.[7,8,2] Clearly, globally distributed, high spatial resolution, and high fidelity atmospheric CO_2 measurement from space is greatly desired for global and regional carbon cycle studies.

In the past decade, some efforts have been made to study the possibility of monitoring atmospheric CO_2 from space.[9,10,11] More recently O'Brien and Rayner[12] and Kuang et al.[13] have addressed this issue using a similar presumed measurement strategy to that which we use here. This study is another effort to explore the feasibility of space-based global measurement of atmospheric total column CO_2 – a quantity that can be used to estimate the sinks and sources of CO_2 at the Earth's surface. In preliminary studies, we examined several potential CO_2 absorption bands, and decided to pick the 1.58 μm band as the optimal one because the solar flux is higher at this wavelength than at longer wavelengths and because inference from other species is minimal. However, the overall findings from this analysis at 1.58 μm will apply as well to other CO_2 vibration-rotational bands in the solar infrared, e.g., 2.0μm, and 1.61μm. This paper first describes the basic radiation features of this band for the realistic atmosphere with both absorption and scattering, and then presents the results of calculations of the back-to-space radiances for the boundary layer CO_2 amount changing under various geophysical conditions (i.e., solar zenith angle, water vapor, aerosols and clouds). The dependence of the radiance sensitivity on atmospheric temperature profile and surface pressure data also will be addressed. This study focuses on the general responses of the back-to-space radiances at this band to the boundary layer atmospheric CO_2 change that directly links to the sources and sinks of CO_2. No specific instrumentation is described in this paper and no particular instrument characteristics (i.e., instrument noise, dynamic range) are included in these results. However, the results of this work provide the basis for the future forward model and retrieval algorithm development and illustrate the instrument requirement specifications needed for space-borne instrument development.

Measurement Strategy

Atmospheric carbon dioxide is chemically unreactive and has its main sources and sinks at the Earth's surface. Its concentration is variable in the planetary boundary layer, but at higher levels its mixing ratio is nearly constant below the dissociation level of molecular oxygen (~ 90 km); above this level carbon dioxide dissociates and its concentration is quickly reduced with altitude. It is a well-mixed and long-lived greenhouse gas and shows a consistent long-term trend at the different observatories across the hemispheres for the past half century (http://www.cmdl.noaa.gov/ccgg/).[14] However, its concentration has strong local and seasonal variability. At ground level, its seasonal cycle is highest in the Northern Hemisphere high latitudes (i.e., 12-22 ppmv), decreases southward (i.e., ~8 ppmv at mid-latitudes, ~4 ppmv at the Equator) and reaches only 1- 2 ppmv in the southern hemisphere.[6] CO_2 variability is rapidly damped with altitude above the boundary layer. Free-troposphere/lower stratosphere vertical gradients are typically about 1% (3-4 ppmv).[15,16]

Because most of the variability in atmospheric CO_2 occurs in the planetary boundary layer, measurement of the total column CO_2 can well represent CO_2 variability related to sinks and sources provided the measurement is of sufficient precision. Such measurement should be precise enough to resolve CO_2 seasonal variability and horizontal gradients, averaged on a typical grid box (i.e., 1x1°) and time scale (i.e., monthly) for climate studies, and accurate enough to be able to resolve long-term trend. For a column average, the mixing ratio gradients over horizontal scales of about 1000 km are typically 1 to 3 ppmv.[17] The column measurement goal of 1 ppmv precision on a time scale of 1 month has been shown to significantly improve surface source/sink estimates in model studies.[7,8]

Radiance measurement from space at a CO_2 absorption band can reflect the total column CO_2 amount. There are several major CO_2 absorption bands in the incoming solar radiation and outgoing atmospheric thermal emission. The strong CO_2 emission bands at 15 μm and 4.3 μm are

used to derive atmospheric temperature profiles[18,19,20], with an assumption that the CO_2 concentration through the whole atmosphere is fixed.[21,22] The sensitivity of space observed radiance to emission temperature in both bands is much larger than the sensitivity to CO_2 concentration change. In addition, water vapor has significant interference in both bands.

In contrast, the measurement of solar radiation absorption by CO_2 has much less sensitivity to atmospheric temperature and water vapor, and is expected to have a better chance to detect small atmospheric CO_2 fluctuation. The vibration-rotational CO_2 solar infrared band at 1.58 μm, as shown in Fig. 1, will allow solar radiation to go through the whole atmosphere and be reflected back to space by the Earth's surface. The back-to-space radiance is sensitive to the total column CO_2 abundance. This band has two very regular groups of lines called as the *P*- and *R*-branches to the left and the right, respectively and separated by a gap caused by a missing line at the center of the band at wavenumber 6347.85 cm^{-1}. The absorption lines in each branch are nearly equally spaced. The line space in the higher frequency branch is slightly narrower than that in the lower frequency branch. As shown below, this band has the minimal water vapor (H_2O) interference and provides sufficient radiance signal for atmospheric total column CO_2 detection, compared to other CO_2 bands in the solar infrared. Moreover, there is no other gas interference in this band.

An additional constraint on the space-based measurement strategy comes from the requirement to observe CO_2 changes near the surface. For a near-nadir viewing satellite observation point, the surface spot size must be as small as possible (high spatial resolution, e.g., 10 km or less) to maximize the chance of seeing between clouds to get clear-sky pixels. A small ground spot is difficult to achieve while still meeting the precision/accuracy requirement because the detected upward radiance is reduced as the observed solid angle diminishes. Because the satellite ground track speed from low earth orbit is about 7 km s^{-1}, the requirement for a small ground spot size also translates into a requirement for a rapid measurement sample time, e.g., 1 s or less. This requirement would be greatly relaxed for a geostationary orbit deployment.

Radiative Transfer Calculations

The radiative transfer model used in this study for atmospheric absorption is called the Line By Line Radiative Transfer Model (LBLRTM), which is from Atmospheric and Environmental Research, Inc., in Cambridge, Massachusetts.[23,24] The heritage of LBLRTM lies in FASCODE[25] developed at the Air Force Phillips Laboratory. LBLRTM is an accurate, efficient and well-validated line-by-line code that is broadly used in atmospheric radiation and remote sensing for the validation of band models, the generation of fast forward models in the retrieval process, and radiance simulation for high spectral resolution sensor design. The High-resolution TRANsmission (HITRAN[26]) molecular absorption database is used as input to LBLRTM. Voigt profile[27] is used for absorption line shapes in order to include both collision- and Doppler-broadening processes in the whole column of atmosphere. The high-resolution incident solar irradiance spectrum is taken from the Kurucz[28] compilation for the full solar disk.

Scattering, including multiple scattering, is computed with the Discrete Ordinates Radiative Transfer (DISORT) model.[29] DISORT has been provided to the community for years for time-independent radiative transfer calculations in vertically inhomogeneous, non-isothermal, plane-parallel media with the physical processes including thermal emission, scattering, absorption, and bi-directional reflection and emission at the lower boundary. It has been implemented in the band models, i.e., MODTRAN, and now for the first time is implemented into the line-by-line model (LBLRTM) for this research. The recent version 2.0 of DISORT is used in the following calculations, which include the both the delta-M transformation of Wiscombe[30] and the intensity corrections of Nakajima and Tanaka[31] to achieve optimum computational efficiency and accuracy for strongly forward-peaked phase functions. For balance between accuracy and computing time, 32-stream angular calculation is performed in this study.

The US Standard Atmosphere 1976 is used for atmospheric profiles with extension up to 120 km. The model atmosphere is assumed to be plane-parallel and divided into total 60 layers.

The vertical resolution of the layers is from 0.7 km in the lower troposphere to 5 km in the middle stratosphere. Each layer is considered as a homogeneous path in the calculations and its temperature and pressure are represented by density weighted mean values with the effects of refraction and the Earth's curvature included.

Incoming solar radiation is attenuated as it penetrates the atmosphere, reflects from the surface and travels back to space. In the real atmosphere, the attenuation at the 1.58 μm band includes the molecular (Rayleigh) scattering, absorption by CO_2 and other gases such as H_2O, extinction (scattering plus absorption) by aerosols and transmissive cirrus clouds, and partial reflection at the Earth's surface. As illustrated in Fig. 2, the total radiance back to space toward the sensor, I, consists of five components. I_{dir} is the direct solar beam reflected toward the sensor Field-Of-View (FOV) by Earth's surface. I_{bsct} is the back-scattered light from the atmosphere including aerosol and clouds (also called the atmospheric backscattering). I_{srfl} is the scattered light reflecting from surface. I_{rsct} is the surface reflected light out of the sensor FOV which is then scattered toward the sensor, and I_{msct} is the light which has already been scattered by the atmosphere and then scattered again toward the sensor or so-called multiple scattering,

$$I = I_{dir} + I_{bsct} + I_{srfl} + I_{rsct} + I_{msct} . \qquad (1)$$

Each component in the equation is strongly frequency dependent owing to the CO_2 absorption features.

The scattered solar radiances, I_{bsct}, I_{srfl}, I_{rsct} and I_{msct}, will have different paths than the direct beam I_{dir} toward sensor, as shown in Fig. 2, and thus will affect total column CO_2 absorption and the radiance sensitivity to CO_2 changes in the atmosphere. Among these components, the atmospheric backscattering I_{bsct} will not hit the surface, thus will lessen total column absorption and also will not be sensitive to CO_2 change beneath. On the other hand, the forward scattering components, I_{srfl}, I_{rsct} and I_{msct}, overall go through longer paths than the direct beam and thus enhance CO_2 absorption and radiance sensitivity. The net effect of these

components depends on the optical characteristics and vertical distribution of scattering media (aerosols/cirrus clouds), surface properties and solar/satellite zenith angles as well. In the presence of significant amount of aerosols and/or cirrus clouds in the atmosphere, on a dark surface, the atmospheric backscattering I_{bsct} is dominant in the total radiance measurement I; on a bright surface, the surface reflected contributions, I_{dir}, I_{srfl} and I_{rsct}, are dominant.

In retrieval practice, the ratio of measured radiances at a weak absorption (so-called off-line) channel and a strong absorption (so-called on-line) channel is used to estimate column CO_2 without retrieving surface reflectance.[32,12] Following is an illustrative analysis showing how the atmospheric scattering affects off-line to on-line radiance ratio that may result in an overestimate or underestimate of column CO_2.

Considering a beam of sunlight, I_0, it goes through five different processes and paths through atmosphere and then toward the sensor, as illustrated in Fig. 2. The direct beam, I_{dir}, at off-line channel ν_{off} can be expressed by

$$I_{dir}^{\upsilon_{off}} = r_s I_0 e^{-(\tau^{\upsilon_{off}} + \tau_{cld})(\frac{1}{\mu_0}+\frac{1}{\mu_1})}, \qquad (2)$$

where r_s is surface reflectance, $\tau^{\upsilon_{off}}$ is the optical thickness of CO_2 along a vertical path from surface to space, τ_{cld} is the optical thickness of cloud that could be aerosols or cirrus, $\mu_0=\cos(\theta_0)$, θ_0 is solar zenith angle, $\mu_1=\cos(\theta_1)$, θ_1 is satellite zenith angle, which equals 1 at nadir viewing. Here, I_0, r_s and τ_{cld} are assumed to be constants within this narrow band. Similarly, at on-line channel ν_{on},

$$I_{dir}^{\upsilon_{on}} = r_s I_0 e^{-(\tau^{\upsilon_{on}} + \tau_{cld})(\frac{1}{\mu_0}+\frac{1}{\mu_1})}. \qquad (3)$$

Then, the (observable) ratio between off-line and on-line is

$$c_0 = \frac{I_{dir}^{\upsilon_{off}}}{I_{dir}^{\upsilon_{on}}} = e^{\Delta\tau\ (\frac{1}{\mu_0}+\frac{1}{\mu_1})}, \qquad (4)$$

where $\Delta\tau = \tau^{\upsilon_{on}} - \tau^{\upsilon_{off}}$ represents the differential absorption of CO_2 between the on-line and off-line channels, which is directly related to total column amount.

For the scattered light I_{srfl}, at channel ν_{off} and ν_{on}, respectively,

$$I_{srfl}^{\upsilon_{off}} = r_s I_0 \omega_{off} p(\mu_d) e^{-(\tau^{\upsilon_{off}}+\tau_{cld})(\frac{1}{\mu_0}+\frac{1}{\mu_1})} e^{-\tau_l^{\upsilon_{off}}(\frac{1}{\mu_d}-\frac{1}{\mu_0})}, \qquad (5)$$

$$I_{srfl}^{\upsilon_{on}} = r_s I_0 \omega_{on} p(\mu_d) e^{-(\tau^{\upsilon_{on}}+\tau_{cld})(\frac{1}{\mu_0}+\frac{1}{\mu_1})} e^{-\tau_l^{\upsilon_{on}}(\frac{1}{\mu_d}-\frac{1}{\mu_0})}, \qquad (6)$$

where $\tau_l^{\upsilon_{off}}$ and $\tau_l^{\upsilon_{on}}$ are the optical thickness of CO_2 below cloud layer for channel ν_{off} and ν_{on}, respectively, μ_d=cos(θ), θ is the zenith angle of downward scattering, and $p(\mu_d)$ is the scattering phase function at this angle. The single scattering albedo of the cloud layer (mixed with absorbing gas CO_2) is

$$\omega_{off} = \frac{k_{sct}^{cld}}{k^{\upsilon_{off}} + (k_{abs}^{cld} + k_{sct}^{cld})}, \text{ and } \omega_{on} = \frac{k_{sct}^{cld}}{k^{\upsilon_{on}} + (k_{abs}^{cld} + k_{sct}^{cld})},$$

where $k^{\upsilon_{off}}$ and $k^{\upsilon_{on}}$ are CO_2 absorption coefficients at channel ν_{off} and ν_{on}, respectively, in the cloud layer. Thus the ratio between the two is

$$c_1 = \frac{I_{srfl}^{\upsilon_{off}}}{I_{srfl}^{\upsilon_{on}}} = \frac{k^{\upsilon_{on}} + k_{ext}^{cld}}{k^{\upsilon_{off}} + k_{ext}^{cld}} e^{\Delta\tau\ (\frac{1}{\mu_0}+\frac{1}{\mu_1})} e^{\Delta\tau_l(\frac{1}{\mu_d}-\frac{1}{\mu_0})}, \qquad (7)$$

where $k_{ext}^{cld} = k_{abs}^{cld} + k_{sct}^{cld}$ is the cloud extinction coefficient, and $\Delta\tau_l$ is the optical thickness difference between the two channels below the cloud layer. The ratio change in comparison with the direct beam can be expressed as

$$\Delta c_1 = \frac{c_1 - c_0}{c_0} = c_\omega e^{\Delta\tau_l (\frac{1}{\mu_d} - \frac{1}{\mu_0})} - 1. \quad (8)$$

Here, $k^{\upsilon_{on}} > k^{\upsilon_{off}}$, so the single scattering albedo ratio, $C_\omega = (k^{\upsilon_{on}} + k_{ext}^{cld})/(k^{\upsilon_{off}} + k_{ext}^{cld})$ is always greater than 1. Then the sign of the ratio change depends on the scattering path length differential against the direct beam. When the scattering goes through a longer path length than the direct beam, $(1/\mu_d - 1/\mu_0) > 0$ and $\exp[\Delta\tau_l (\frac{1}{\mu_d} - \frac{1}{\mu_0})] > 1$, thus $\Delta c_1 > 0$, which means the scattering enhances CO_2 absorption and leads to an overestimate of column CO_2 amount. When the path length change $(1/\mu - 1/\mu_0) < 0$ and thus $\exp[\Delta\tau_l (\frac{1}{\mu_d} - \frac{1}{\mu_0})] < 1$, the Δc_1 sign could be negative or positive, depending the magnitude of the path length change and single scattering albedo ratio c_ω.

Similarly, the off-line to on-line radiance ratio change of I_{rsct} relative to the direct beam I_{dir} can be expressed as

$$\Delta c_2 = c_\omega e^{\Delta\tau_l (\frac{1}{\mu_u} - \frac{1}{\mu_1})} - 1, \quad (9)$$

where $\mu_u = \cos(\theta)$, θ is the zenith angle of upward scattering. Δc_2 has the same sensitivity feature as Δc_1, described above.

For the backscattering component I_{bsct}, the ratio change in regard to I_{dir} is

$$\Delta c_3 = c_\omega e^{-\Delta\tau_l (\frac{1}{\mu_0} + \frac{1}{\mu_1})} - 1. \quad (10)$$

In this case, $\exp[-\Delta\tau_l (\frac{1}{\mu_0} + \frac{1}{\mu_1})]$ is always less than 1. For high altitude cirrus clouds, $\Delta\tau_l$ can be large enough to make Δc_3 negative and thus lead to an underestimate of column CO_2. For aerosols in the lower atmosphere when $\Delta\tau_l << 1$, Δc_3 still could be positive and cause a positive

bias in column CO_2 retrieval. Over dark surfaces, I_{bsct} is large relative to I_{dir} and the Δc_3 effect dominates.

The expression of ratio change for multiple scattering I_{msct} is more complicated. As an example, the twice-scattered light as illustrated in Fig. 2, the ratio change can be expressed as

$$\Delta c_4 = c_\omega e^{\Delta\tau_l[(\frac{1}{\mu_u}-\frac{1}{\mu_1})+(\frac{1}{\mu_d}-\frac{1}{\mu_0})]} - 1, \qquad (11)$$

which is usually positive. Overall, the net influence of aerosols and/or cirrus clouds depends on the integral of Δc_1, Δc_2, Δc_3 and Δc_4 over all atmosphere layers and over whole sensor FOV that will be calculated and discussed case by case in the following results.

In this study, three different sky conditions are tested in the calculations: clear, cloudy and hazy sky. In the real world, there are always very small particles suspended in the air even for the so-called clear sky. As a baseline, the clear sky here is defined as the clear condition with fine background aerosols. In the troposphere, the LOWTRAN troposphere aerosol model with 50 km visibility (VIS) is applied.[33] The LOWTRAN background aerosol models for the upper atmosphere up to 100 km are also included. So in the baseline calculations, extinction by those atmospheric background aerosols as well as the molecular scattering are all accounted even though the molecular scattering at this frequency is negligible. The atmospheric thermal emission at this frequency is neglected here. For the separation of CO_2 signal from others, the water vapor absorption is not included in all the baseline and perturbation runs, but its interference in this band will be calculated and discussed separately below.

Clouds cover roughly half the Earth. Among all kinds of clouds, the upper troposphere transmissive cirrus cloud has the highest probability of occurrence. The statistics of 4-year High-resolution Infrared Radiation Sounder (HIRS) cloud data show that on average the frequency of cirrus clouds is about 40%.[34] Cirrus clouds are normally located in the upper troposphere and are predominantly composed of columnar crystals. In this study, the LOWTRAN standard cirrus

model[33] is added to the baseline atmosphere, with 1 km thickness and 10 km base height. The clouds are composed of ice crystals with a 64-μm effective radius, which gives a size parameter of 250 at 1.58 μm for Mie scattering. The asymmetry factor of these cirrus ice crystals calculated using Mie theory is 0.93 at this wavelength. In reality, the cirrus cloud particles are not spherical, more likely hexagonal column, and the asymmetry factor determined for equivalent spheres is uniformly larger than for hexagonal ice crystals.[35] A factor of 0.85 has been recommended to multiply the asymmetry factor value derived from Mie theory for equivalent ice spheres to account for the effect of particle shape on scattering.[36] In this study, the same factor is used, adjusting the asymmetry factor of this cirrus cloud to about 0.8, which still indicates a highly forward scattering.

In the calculations for hazy conditions, coarse aerosols are added in the atmospheric boundary layer below 2 km. All the aerosol models used here are also taken from LOWTRAN.[33] Three aerosol extinctions are tested in this study. The first one is the rural extinction with meteorological range of 23 km visibility. This rural aerosol model is intended to represent the average aerosol condition over continents where there is no direct influence of urban and/or industrial aerosol sources. The second one is the urban extinction with 5 km visibility meteorological range, which is the mixture of the rural aerosols with soot-like aerosols. The third is the maritime extinction with meteorological range of 23 km visibility, which is representative for the boundary layer atmosphere over the oceans. The asymmetry parameter is calculated using Mie theory[37] for each aerosol type, and the Henyey-Greenstein phase function[38] is used for all aerosol cases as well as the cirrus cloud case. The optical features of these aerosols as well as cirrus clouds are all assumed to be constant in this 17-nm band. Table 1 lists the optical characteristics of these three types of aerosols and cirrus cloud used in this study.

The earth's surface is treated as Lambertian (i.e., the reflected radiation is assumed to be unpolarized and isotropic) in the calculations. The spectral reflectance for the 1.58 μm band is assumed to be a fixed value of 0.3. These assumptions represent global average surface

conditions so that the sensitivity results based on such conditions have general representation. Surface reflectance of 0.3 is considered a reasonable value over land (i.e., for generic vegetation and bare soil[39]) at this wavelength. Over oceans, the surface reflectance is usually less than 0.1 for solar zenith angle less than 65°.[40] At larger solar zenith angle, the reflectance over ocean could reach 0.3 or greater. The reflectance could be greater than 1.0 for sun glint, when satellite view zenith angle equals to the solar zenith angle and satellite view azimuth angle equals to the solar azimuth angle plus 180 degree. The novel approach of using the sun glint to monitor the CO_2 variation over ocean for the 2/3 of the global surface is strongly recommended.[7,9] The use of the sun glint over ocean can significantly increase the signal-to-noise ratio of the radiance measurement, which is critical to high precision requirement of atmospheric CO_2 measurement. It will also change the instrument dynamic range. Obviously, the cost of using the sun glint technique is a significant loss of spatial coverage that may be affordable for 1°x1° monthly mean data requirement.

Results

(a). Spectral Resolution

The molecular absorption line width for CO_2 vibration-rotation bands is fairly constant, with a value of about 0.07 cm^{-1} for a reference temperature T_0=273 K and pressure P_0=1013 mbar.[26] Here, a triangle scanning function is used to convolve the line-by-line calculated monochromatic radiances. Radiance measurement of the reflected solar infrared at very high spectral resolution may give high sensitivity to atmospheric CO_2 change, but has low signal level (~ very opaque) and low signal-to-noise ratio. On the other hand, the measurement at very low spectral resolution may show too little sensitivity to detect the small amount of CO_2 change in the lower atmosphere. Therefore the spectral resolution and radiance sensitivity should be well balanced in instrumentation for space-based CO_2 measurement. After a set of experiments, a 0.035 cm^{-1} output spectral resolution with a 0.07 cm^{-1} Full-Width-Half-Maximum (FWHM) scanning

function is considered to be a good choice. Figure 3 demonstrates the impact on radiance and radiance sensitivity to changing spectral resolution from the model possible highest (~0.0014 cm^{-1}) to a coarse 0.5 cm^{-1}. Obviously 0.07 cm^{-1} resolution can resolve CO_2 spectral features, maintain the moderate radiance level, and have good radiance sensitivity.

The following results are all based on this resolution and for the wavenumber range 6315-6385 cm^{-1}. It is noteworthy that the radiance structure for both branches shown in Fig. 3 is not as regular as that shown in the transmittance plot in Fig. 1. The details of the incoming solar irradiance structure are included in the back-to-space radiances. The baseline atmospheric CO_2 mixing ratio is set to be 360 ppmv and the satellite is chosen to be nadir viewing. Solar zenith angle is chosen to be a moderate value of 30 degree. Table 2 lists the baseline input and output parameters of radiance simulations.

(b). Radiance Detection Sensitivity

The global atmospheric CO_2 concentration has increased by about 1.5 ppmv per year in the 1990s.[1] When the atmospheric CO_2 mixing ratio increases by 1 ppmv (~0.28%) uniformly in the whole column, the back-to-space solar infrared radiance decreases up to 0.38% (at 0.07 cm^{-1} spectral resolution), as shown in the bottom panel of Fig. 3. Obviously, the radiance change is proportional to the CO_2 absorption, and, on average, it is close to a one-to-one correspondence near the line centers.

The goal of the space-based column atmospheric CO_2 measurement is to globally quantify the near-surface variability and gradients and thus to estimate the global and regional carbon budget. So this sensitivity study focuses on the CO_2 perturbation in the atmospheric boundary layer. Figure 4 shows the radiance change corresponding to a 1% (~3.6 ppmv, equivalent to seasonal variability of CO_2 at the equator) CO_2 concentration increase in the model atmosphere boundary layer (0-2 km). The change of CO_2 molecular column amount corresponding to 1% CO_2 concentration change in the boundary layer is about 80% of the change

corresponding to a 1 ppmv mixing ratio change in the whole column (above). The radiance change at the top of the atmosphere is correspondingly about 70% near the line centers (c.f., Figures 3 and 4). In comparison, the Rayleigh scattering is about one order of magnitude smaller than this radiance change. The median radiance sensitivity to the 1% CO_2 concentration increment in the boundary layer over the band is about 0.15%. This implies that the instrument signal-to-noise (SNR) ratio should be at least 700:1 in order to detect 1% CO_2 change near the Earth's surface on a single sample basis. Presumably, in the retrieval process an instrument that measured across multiple CO_2 lines would be able to reduce the statistical (photon counting) detection noise by approximately the square root of the number of lines. Beyond this, the random variations in signal would be further reduced by averaging individual measurements into area/temporal averages, e.g., monthly 1°x1°. It is not known, however, how much precision will be improved by averaging individual measurements taken under different geophysical conditions. Systematic measurement errors (bias) must be extremely small to accurately infer information about surface fluxes from CO_2 concentration measurements.[7]

Measurement of reflected solar radiance at high latitudes faces the large solar zenith angle, low light conditions that imply low SNR. At a solar zenith angle of 80^0 the solar insolation (the solar flux incident on a horizontal unit area) at the top of the atmosphere is about 1/5 that at 30° while the optical path through the atmosphere to the ground is 5 times larger. Thus, the back-to-space radiances are correspondingly only 1/5 of those at 30 degree in the wings where there is only small absorption, and as little as 1/40 in the peak line centers, shown in the top panel of Fig. 5. However, the radiance sensitivity to the 1% CO_2 concentration increment in the boundary layer is almost doubled near the line centers, shown in the bottom panel of Fig. 5. Although sensor dynamic range and signal-to-noise ratio could be a problem, remote sensing of CO_2 at high solar zenith angles, characteristic of high latitudes or near dawn and dusk for peak-to-peak diurnal variability, for example, could be feasible. One advantages of the measurement at high latitudes

is the higher surface reflectance (i.e., of ice), however clouds are more likely to obscure the surface at low sun angles.

(c). Sensitivity in Retrieval

The radiance ratio between an off-line and an on-line channel that represents CO_2 absorption is usually used to retrieve column CO_2 abundance without retrieving complicated surface reflectance.[32,12] However, the scattering of aerosols and/or cirrus clouds in the atmosphere can modify such radiance ratio, even though the aerosol/cirrus cloud properties are constant in this band. As described in the previous section, such modification is caused by the differential path length of scattering from direct beam and differential absorption between off-line and on-line of CO_2. Our calculations show these effects could cause large systematic retrieval error. The magnitude and even sign of the systematic retrieval error is a function of the optical characteristics and vertical distribution of aerosols/cirrus clouds, surface properties, and solar and satellite zenith angles as well.

Figure 6 shows the radiance ratio changes from baseline for the 1% CO_2 perturbation in the boundary layer and for the aerosol and cirrus cloud cases used in the calculations. The ratio changes are positive for all the cases, which indicates that generally aerosols and cirrus clouds will enhance CO_2 absorption and lead to an overestimate of column CO_2 amount. This finding differs somewhat from the corresponding figure and discussion for cloud and aerosol scattering effects from O'Brien and Rayner[12], who show a decrease in off/on-line ratio for the cirrus scattered component of the radiation and little change for aerosol (their figure 3). In the discussion, they stressed an underestimate in CO2 resulting from scattering, e.g., clouds screen absorption by CO2 in the underlying atmosphere (Note, however, that the apparent CO2 change due to the presence of scattering (their table 1) is positive consistent with our calculations although there are several other differences in simulated conditions). The main reason for enhanced CO_2 absorption in the presence of clouds and aerosol is that the 0.3 surface reflectance

is bright enough to make the surface-reflected forward scattering larger than backscattering in the total diffused radiance toward the sensor, and thus lengthening the overall path of the sunlight.

Table 3 gives an example of the relative contributions of direct and diffused components in total back-to-space radiances and their impact on the radiance ratio at two adjacent frequencies near the center of the R-branch for the cirrus cloud case. The surface reflected scattered radiances, sum of I_{srfl}, I_{rsct} and I_{msct}, increase the total radiance ratio and result in an overestimate of column CO_2 for this case. I_{bsct} is only 1.5% of the back-to-space radiance offline and 3.7% online.

High-altitude and highly forward scattering cirrus clouds and bright maritime aerosols have the largest impact on the radiance ratio, up to around 1%, which is equivalent to a 4% or 15-ppmv CO_2 change in the boundary layer. For rural aerosols, such impact is about comparable to the 1% or 4-ppmv change of CO_2 concentration near surface (Figure 6). Only the effect of absorptive urban aerosols is relatively small, equivalent to about 1 ppmv CO_2 change in the boundary layer, even though the urban aerosols have the largest optical thickness among the cases.

It is obvious that any ancillary simultaneous co-located aerosols/cirrus cloud data and even surface property data are critically useful to narrow CO_2 retrieval uncertainty. Further radiance calculations showed that among the optical characteristics of aerosols/cirrus clouds listed in Table1, radiance ratios are more sensitive to uncertainties in single scattering albedo and asymmetry parameter (or phase function) than the amount of aerosols/cirrus clouds or optical thickness. For example, in the cirrus case the retrieval error due to 5% uncertainty in either single scattering albedo or asymmetry parameter data is twice as large as that caused by 5% uncertainty in optical thickness data. Similarly, in hazy conditions it is critical to precisely specify the aerosol type in CO_2 retrieval. Fine and absorptive aerosols, e.g., industrial pollutants, have minor impact on column CO_2 retrieval. However, the large and bright aerosols such as sea salts and dusts could lead to a large bias in retrieval.

The magnitude and sign of such bias in retrieval depends on overall features of aerosols/cirrus, Earth's surface property and solar/satellite geometry. For example, the calculations with perturbed asymmetry parameter g for the cirrus case shows that when cirrus g is slightly less than 0.7 the retrieval using these two adjacent channels has nearly zero bias, shown in Table 4. At this point, the differential path length effect and differential single scattering albedo effect from all scattering components, as described in previous section, are nearly canceled overall. For less forward peaked scattering (g=0.5 or 0.6), I_{bsct} dominates leading to decreased absorption by CO_2.

Calculations for the tested cirrus and hazy conditions, listed in Table 1, showed that the radiance sensitivities to the boundary layer CO_2 change in all these four cases are almost unchanged from the baseline, maintaining about 0.25% level at peak. This result indicates that the effect of the net path length modification by cirrus or aerosol scattering is small in terms of precision in detecting boundary layer CO_2 gradients, provided the aerosol properties are constant over the region in question, consistent with the analysis of Kuang et al..[13] In summary, we concur with previous analyses from O'Brien and Rayner[12] and Kuang et al.[13] that highly sensitive detection of CO_2 may be possible in the presence of optically thin clouds and aerosols if additional information about photon path is provided, e.g., through O_2 measurements, but the dependence of the scattering effects on surface and particle properties, which are not in general independent of wavelength, leads us to a clear recommendation that retrieval methods need to incorporate additional information about aerosols. This would best be accomplished by including aerosol sensors with the CO_2/O_2 spectrometer or possibly by using measurements from other sensors, e.g., MODIS (Moderate Resolution Imaging Spectrometer), CALIPSO (Cloud-Aerosol Lidar and Infrared Pathfinder Satellite Observations), etc.

(d). Temperature Dependence

The CO_2 molecular absorption coefficient significantly depends on temperature in terms of line strength, line shape and even line position.[41] Therefore, the amount of back-to-space radiance in the solar infrared depends on atmospheric temperature profile, even though the dependence is much weaker than in the atmospheric thermal infrared (i.e., 4.3 and 15 μm CO_2 bands). Our calculations show that the atmospheric temperature profile seasonal variability (e.g., change from mid-latitude summer to winter) will cause back-to-space radiance change up to a few percent in the absorption line centers. Synoptic variations in temperature can be tens of degrees. So ancillary temperature profile data must be input to the CO_2 retrieval processing in real-time, instead of using any temperature climatology, in order to achieve measurement precision of less than 1%.

The development of the space-based temperature profile sounder has made great progress in the past few years. Future sounders have thousands of channels compared to only 20 channels in the current operational sounder TOVS (TIROS-N Operational Vertical Sounder). The temperature retrieval RMS error for the AIRS instrument on Aqua should be better than 1 K in 1-km thick layers from the surface to 300 mbar, 3-km thick layers from 300 mbar to 30 mbar and 5-km layers from 30 mbar to 1 mbar.[42] In this study, 1 K temperature deviation is added to every layer of the U.S. standard atmosphere. The signs of the error are randomly generated for each vertical layer, which is likely for temperature profile retrieval errors in matching the observed radiances with computed radiances. Note that assuming a climatological temperature profile would produce much larger errors in temperature, up to 10 K. Fig. 7 shows the radiance change in percentage after the 1 K RMS error is introduced in the temperature profile. The overall influence of the temperature retrieval error is less than 0.05%, significantly smaller than the change due to 1% CO_2 change in the boundary layer. The population of the molecular lines systematically shifts with changing temperature. This feature gives a great advantage to removing the large part of the temperature influence in the column CO_2 retrieval by using multiple channels in this band, compared to using just single pair of off-line and on-line channels.

(e). Water Vapor Interference

Water vapor has slight absorption in this solar infrared band, as seen in Fig. 1. But it can change the back-to-space radiance up to a few percent at its line centers, shown in Fig. 8. This requires attention when channels are selected for CO_2 retrieval. Fortunately, most of water vapor line centers in this band are not aligned with CO_2 line centers. The difference in CO_2 sensitivity with and without water vapor is shown to be negligible in our calculations for most lines. Therefore, very minor interference with quite variable atmospheric water vapor is a great merit of this solar infrared band in comparison with other CO_2 solar bands, such as 2.7 and 2.0 μm bands.

(f). Surface Pressure Requirement

Two aspects of the effect of changing surface pressure on CO_2 detection are discussed here. In the first, model simulations show that variations in terrain height and surface pressure can create gradients in total column CO_2 larger than those induced by surface CO_2 flux variations.[17] Thus surface pressure should be provided in order to separate the contribution due to the atmospheric column density variation from the signal due to atmospheric CO_2 mixing ratio changes. The total column CO_2 then should be normalized for local terrain height in order to properly interpret horizontal gradients of CO_2 with regard to sources and sinks.

There are thousands of ground sites worldwide measuring surface pressure at least twice a day. But the coverage of the data over oceans, in the southern hemisphere, and in mountainous areas (i.e., the Tibetan Plateau) is poor. Unfortunately, to date there is no space-based instrument to globally measure this parameter, even though many efforts have been made in the development of such instruments using oxygen (O_2) A-band.[43,44,45,46] Even over the land with an adequate number of ground sites, because of the mismatch between the ground observations of surface pressure and space-based measurement of CO_2 in timing and geo-location, the precision of surface pressure data, if from a global weather forecast model (i.e., NCEP model), is estimated to

be several mbar. Kuang et al.[13] advocate the use of collocated O_2 A-band (760 nm) measurements while O'Brien and Rayner[12] suggest using the O_2 Delta-band (1270 nm) because it is nearer the CO_2 wavelengths, although subject to airglow emissions. In either case, the O_2 measurement must observe at precisely the same place and time as CO_2 to achieve high precision.

The second aspect of changing pressure is the impact on the CO_2 absorption line width through pressure broadening. Our calculations show the radiance changes due to 2-mbar surface pressure fluctuations (~the possible accuracy achievable from O_2 sensor[43]) are less than 0.01%, at least one order less than the changes due to 1% CO_2 concentration change in the lower atmosphere.

Conclusion and Discussions

A series of sensitivity studies have been performed to explore the feasibility of space-based global CO_2 measurement for global and regional carbon cycle study. The results indicate that the relatively small amount of CO_2 variation near the Earth's surface may be detected in the radiance measurement of reflected solar infrared at 1.58 μm. The results were calculated using the line-by-line radiative transfer model and presented at a 0.07 cm-1 spectral resolution, the typical line width of CO_2 at standard temperature (T_0=273K) and pressure (p_0=1013 mbar), in order to fully resolve the line features and achieve maximum radiance sensitivity near the surface where the main CO_2 sources and sinks are located. In this spectral resolution, the requirement of sensor signal-to-noise ratio is at least 700:1 for detecting the signal of a 1% CO_2 concentration change in the atmospheric boundary layer at current 360-ppmv levels. The requirement for detecting a 1 ppmv change in the total column CO_2 is about 500:1.

Water vapor has minor interference overall in this solar infrared band. However, when aerosols and/or cirrus clouds are present in the atmosphere, scattering by the particles will modify the sunlight path length and thus change total column CO_2 absorption. Our full radiative transfer calculations show that for typical cases the net effect of scattering on radiance sensitivity to near-

surface CO_2 is negligible, i.e., the screening effect of cirrus and aerosol on detection of CO_2 changes in the lower atmosphere is small. However, such scattering influence will lead to systematic errors in retrieval of column CO_2 amounts if the aerosols or cirrus cloud scattering is unknown. The magnitude and sign of this error depends on the scattering and absorption characteristics of the particles, surface reflectivity, and the solar observation geometry. Simultaneous co-located aerosols/cirrus clouds data and surface albedo data as well are paramount to CO_2 retrieval at high precision. Approaches to minimize the scattering effect on differential absorption measurement for CO_2 retrieval are under investigation.

Meanwhile, good knowledge of the atmospheric temperature profile is required as ancillary data in the CO_2 retrieval. The recently launched global atmospheric temperature profilers should meet this requirement. Using multiple channels in the CO_2 band can further minimize temperature dependence.

In additional to the atmospheric temperature profile, the atmospheric column density is needed for analysis of the CO_2 data. Surface pressure must be known to similar precision as the CO_2 column (<1%) in order to isolate the change in column CO_2 owing to surface flux versus that from surface pressure change. The use of surface pressure information from a global weather analysis model may be adequate over land. However, over the oceans and in remote regions collocated data is required from a space-based instrument attached to the CO_2 sensor. The results of similar sensitivity studies, to explore the feasibility of surface pressure measurement from space using reflected sunlight at O_2 A-band near 0.76 μm, will be presented in a separate paper in the near future.

Several potential instrument techniques have been suggested to meet the sensitivity requirements discussed here. For example, the high-resolution grating spectrometer, Michelson interferometer, and Fabry-Perot interferometer are potentially appropriate to the global measurement of CO_2 from space. A grating spectrometer or Michelson interferometer with spectral resolution and signal-to-noise comparable to that used in our calculations can capture the

detailed spectral features of the band and well-selected channels from this type of sensor could permit the generation of high precision CO_2 retrieval.[13] The Michelson interferometer, however, requires a significant amount of time to construct the complete spectrum, relative to the satellite ground track speed (~7 km/s). Therefore this technique would not be well suited to low earth orbit deployment because of low spatial resolution and smearing that would occur, but could be suited to geostationary orbit. Although we have concentrated on CO_2 detection using reflected sunlight, similar detection can possibly be obtained with active sensing using a laser light source. Grating, Fabry-Perot, and laser approaches that satisfy the sensitivity criteria derived here are currently being pursued for potential space deployment.

Acknowledgements

We would like to acknowledge helpful discussions with W. R. Heaps, A. E. Andrews, P.K. Bhartia, and W. Wiscombe of NASA GSFC and funding support from Carbon Cycle Science at NASA.

References

1. R. T. Watson and Intergovernmental Panel on Climate Change (IPCC), Climate Change 2001: Synthesis Report: Third Assessment Report of the Intergovernmental Panel on Climate Change, Cambridge University Press, New York, 2001.

2. P. P. Tans, I. Y. Fung, and T. Takahashi, "Observational constraints on the global atmospheric CO_2 budget," Science **247**, 1431-1438 (1990).

3. S. Fan, M. Gloor, J. Mahlman, S. Pacala, J. Sarmiento, T. Takahashi, and P. Tans, "A large terrestrial carbon sink in North America implied by atmospheric and oceanic carbon dioxide data and models," Science **282**, 442-446 (1998).

4. D. Schimel et al., "Contribution of increasing CO_2 and climate to carbon storage by ecosystems in the United States," Science **287**, 2004-2006 (2000)

5. R. B. Myneni et al., "A large carbon sink in the woody biomass of Northern forests," Proc. National Acad. Sci. 98, 14,784-14,789 (2001).

6. T. J Conway, P. P. Tans, L. S. Waterman, and K. W. Thoning, "Evidence for interannual variability of the carbon cycle from the National Oceanic and Atmospheric Administration/Climate Monitoring and Diagnostics Laboratory Global Air Sampling Network," J. Geophys. Res. **99**, 22,831-22,855 (1994).

7. P. J. Rayner and D. M. O'Brien, "The utility of remotely sensed CO_2 concentration data in surface source inversions," Geophys. Res. Lett. **28**, 175-178 (2001)

8. B. C. Pak and M. J. Prather, "CO2 source inversions using satellite observations of the upper troposphere," Appl. Opt. 28, 4571-4574 (2001).

9. T. Aoki, M. Fukabori and T. Aoki, "Trace gas remote sounding from near IR sun glint observation with tunable etalons," in High Spectral Resolution Infrared Remote Sensing for Earth's Weather and Climate Studies, edited by A. Chedin, M. T. Chahine and N. A. Scott, NATO ASI Series **19,** 309-32$_2$ (Berlin Heidelberg, 1993).

10. J. H. Park, "Atmospheric CO_2 monitoring from space," Appl. Opt. **36**, 2701-2712 (1997).

11. B. T. Tolton and D. Plouffe, "Sensitivity of radiometric measurements of the atmospheric CO_2 column from space," Appl. Opt. **40**, 1305-1313 (2001).

12. D. M. O'Brien and P. J. Rayner, "Global observations of carbon budget 2, CO2 concentrations from differential absorption of reflected sunlight in the 1.61 m band of CO2," J. Geophys. Res., 107, 4354 (2002)

13. Z. Kuang, J. Margolis, G. Toon, D. Crisp and Y. Yung, "Spaceborne measurements of atmospheric CO2 by high-resolution NIR spectrometry of reflected sunlight: An introductory study," Geophys. Res. Let. 29,2002

14. National Oceanic and Atmospheric Administration, Climate Monitoring and Diagnostics Laboratory, Carbon Cycle Group (1999), http://www.cmdl.noaa.gov/ccgg/.

15. T. Nakajawa, K. Miyashita, s. Aoki, and M. Tanaka, "Temporal and spatial variations of upper tropospheric and lower stratospheric carbon dioxide," Tellus B **43**, 106-117 (1991).

16. U. Schmidt and A. Khedim, "In situ measurements of carbon dioxide in the winter arctic vortex and at midlatitudes: an indicator of the 'age' of stratospheric air," Geophys. Res. Lett. **18**, 763-766 (1991).

17. S. R. Kawa, D. J. Erickson, S. Pawson, Z. Zhu, "Global CO2 transport simulations using meteorological data from the NASA data assimilation system," J. Geophys. Res., in preparation, 2003.

18. W. L. Smith, "Iterative solution of the radiative transfer equation for temperature and absorbing gas profile of an atmosphere," Appl. Opt. **9**, 1993-1999 (1970).

19. M. T. Chahine, "Inverse problems in radiative transfer: Determination of atmospheric parameters," J. Atmos. Sci. **27**, 960-967 (1970).

20. C. D. Rodgers, "Retrieval of atmospheric temperature and composition from remote measurement s of thermal radiation," Rev. Geophys. Space Sci. **14**, 609-624 (1976).

21. L. M. McMillin and H. E. Fleming, "Atmospheric transmittance of an absorbing gas: A computationally fast and accurate transmittance model for absorbing gases with constant mixing ratios in inhomogeneous atmosphere," Appl. Opt. **15**, 358-363 (1976).

22. H. E. Fleming and L. M. McMillin, "Atmospheric transmittance of an absorbing gas. 2: A computationally fast and accurate transmittance model for slant paths at different zenith angles," Appl. Opt. **16**, 1366-1370 (1977).

23. S.A. Clough, M.J. Iacono, and J.-L. Moncet, "Line-by-line calculation of atmospheric fluxes and cooling rates: Application to water vapor," J. Geophys. Res., 97, 15761-15785 (1992).

24. S.A. Clough and M.J. Iacono, "Line-by-line calculations of atmospheric fluxes and cooling rates. 2: Applications to carbon dioxide, ozone, methane, nitrous oxide, and the halocarbons," J. of Geophys. Res. **100**,16519-16535 (1995).

25. S. A. Clough, F.X. Kneizys, L.S. Rothman and W.O. Gallery, "Atmospheric spectral transmittance and radiance: FASCOD1B," Proceedings of the SPIE 277, 152 (1981).

26. Rothman, L.S., C.P. Rinsland, A. Goldman, S.T. Massie, D.P. Edwards, J.-M. Flaud, A. Perrin, C. Camy-Peyret, V. Dana, J.-Y. Mandin, J. Schroeder, A. McCann, R.R. Gamache, R.B. Wattson, K. Yoshino, K.V. Chance, K.W. Jucks, L.R. Brown, V. Nemtchinov, and P. Varanasi, "The HITRAN Molecular Spectroscopic Database and HAWKS (HITRAN Atmospheric Workstation): 1996 Edition," Journal of Quantitative Spectroscopy and Radiative Transfer **60**, 665-710 (1998).

27. B. H. Armstrong, "Spectrum line profiles: The Voigt function," J. Quant. Spectrosc. Radiat. Transfer **7**, 61-88 (1967).

28. K. Stamnes, S.-C. Tsay, W. Wiscombe and K. Jayaweera, "A Numerically Stable Algorithm for Discrete-Ordinate-Method Radiative Transfer in Multiple Scattering and Emitting Layered Media," Appl. Opt. **27**, 2502-2509 (1988).

29. W, Wiscombe, "The delta-M method: Rapid yet accurate radiative flux calculations," J. Atmos. Sci., 34, 1408-1422 (1977).

30. T. Nakajima, and M. Tanaka, "Algorithms for radiative intensity calculations in moderately thick atmospheres using a truncation approximation," J. Q. S. R. T., 40, 51-69 (1988).

31. R. L. Kurucz, "Synthetic infrared spectra, in Infrared Solar Physics," IAU Symp. 154, edited by D.M. Rabin and J.T. Jefferies, Kluwer, Acad., Norwell, MA (1992).

32. P. F. Ambrico, A. Amodeo, P. D. Girolamo, and N. Spinelli, "Sensitivity analysis of differential absorption lidar measurements in the mid-infrared region," Applied Optics, 39, 6847-6865 (2000).

33. F. Kneizys, E. Shuttle, W. Gallery, J. Chetwynd, L. Abreu, J. Selby, S. Clough, and R. Fenn, "Atmospheric Transmittance/Radiance Computer Code LOWTRAN 6," U.S. Air Force Geophys. Lab. AFGL-83-0187, Hanscom AFB, MA (1983).

34. D. P. Wylie, W. P. Menzel, H. M. Woolf, and K. I. Strabala, "Four years of global cirrus cloud statistics using HIRS," J. Clim., 12, 1972-1986 (1994).

35. Y. Takano and K. –N Liou, "Solar radiative transfer in cirrus clouds. Part I: Single-scattering and optical properties of hexagonal ice crystals," J. Atmos. Sci., 46, 3-19 (1989).

36. Z. Sun and K. P. Shine, "Studies of the radiative properties of ice and mixed –phase clouds," Quart. J. Roy. Meteor. Soc., 120, 111-137 (1994).

37. S. Asano, "Light scattering properties of spheroidal particles," Appl. Opt. 18, 712 (1979).

38. L. G. Henyey and J. L. Greenstein, "Diffuse radiation in the galaxy," Astrophys. J., 93, 70-83 (1941).

39. B. Pinty and M.M. Verstraete, "Extracting information on surface properties from bidirectional reflectance measurements," J. Geophys. Res., 96(D2), 2865-2874 (1991).

40. B. P. Brieglieb, P. Minnis, V. Ramanathan, and E. Harrison, "Comparison of regional clear-sky albedos inferred from satellite observations and model computations," J. Clim. Appl. Meteorol., 25, 214-226 (1986).

41. I. Heaton, "Temperature scaling of absorption coefficients," J. Quant. Spectrosc. Radiat. Transfer **16**, 801-804 (1976).

42. J. Susskind, C. Barnet and J. Blaisdell, "Determination of atmospheric and surface parameters from simulated AIRS/AMSU/HSB sounding data: retrieval and cloud clearing methodology," Adv. Space Res., 21, 369-384 (1998).

43. R. M. Mitchell and D. M. O'Brien, "Error estimates for passive satellite measurement of surface pressure using absorption in the A band of oxygen," J. Atmos. Sci., 44, 1981-1990 (1987).

44. D. M. O'Brien, R. M. Mitchell, S. A. English, G. A. Da Costa, "Airborne measurements of air mass from O_2 A-band absorption spectra," J. Atmos. Ocean. Technol., **15**, 1272-1286 (1998).

45. G. L. Stephens and A. Heidinger, "Molecular line absorption in a scattering atmosphere. Part I: Theory," J. Atmos. Sci., 57, 1599-1614 (2000).

46. A. Heidinger and G. L. Stephens, "Molecular line absorption in a scattering atmosphere. Part II: Application to remote sensing in the O_2 A band," J. Atmos. Sci., 57, 1615-1634 (2000).

Table 1. Optical characteristics of aerosols and cirrus cloud used in the radiance calculations, where, τ is the optical thickness; ω, the single scattering albedo; and g, the asymmetric factor.

Aerosol Type	τ	ω	g
Maritime	0.13	0.98	0.72
Rural	0.05	0.81	0.64
Urban	0.33	0.52	0.63
Cirrus	0.14	0.73	0.8

Table 2. List of baseline input and output parameters of radiance simulations.

Input	Output
1976 US Standard Atmosphere 0-120 km	Band Coverage: 6315-6385 cm^{-1}
CO_2 level: 360 ppmv	Scanning Function: Triangular
Lambertian Surface with Reflectance: R_s=0.3	Spectral Resolution (FWHM): 0.07 cm^{-1}
LOWTRAN Background Aerosols	Spectral Sampling Step: 0.035 cm^{-1}
Solar Zenith Angle: 30°	
Satellite Viewing Angle: Nadir	

Table 3. The direct beam I_{dir}, the sum of scattered radiances, $I_{sct} = I_{bsct} + I_{srfl} + I_{rsct} + I_{msct}$, and the total back-to-space radiances I at a pair of adjacent off-line and on-line channels near R-branch center and the radiance ratios between the off-line and on-line for baseline clear sky and cirrus case, respectively, and the sensitivity of the ratio to the cirrus. The reference atmospheric CO_2 concentration is 360 ppmv. The off-line frequency ν_{off} is 6359.45 cm^{-1} and the on-line frequency ν_{on} is 6359.98 cm^{-1}. The radiance unit is $mW/m^2/cm^{-1}/sr$.

	Baseline			**Cirrus**		
	I_{dir}	**I_{sct}**	**I**	**I_{dir}**	**I_{sct}**	**I**
Off-line (ν_{off})	**5.0292**	**0.2308**	**5.2600**	**3.7085**	**1.1248**	**4.8333**
On-line (ν_{on})	**0.9159**	**0.0406**	**0.9565**	**0.6754**	**0.1985**	**0.8739**
Ratio	**5.4910**	**5.6847**	**5.4992**	**5.4908**	**5.6665**	**5.5307**
Sensitivity (%) ($\Delta R/R_{baseline}$)						**0.573**

Table 4. Same as Table 3 but for cirrus asymmetry parameter perturbation runs.

Channels	Baseline	Cirrus			
		g=0.5	g=0.6	g=0.7	g=0.8
Off-line (v_1)	5.2600	4.8242	4.8247	4.8288	4.8333
On-line (v_2)	0.9565	0.8979	0.8847	0.8772	0.8739
Ratio (R)	5.4992	5.3728	5.4535	5.5048	5.5307
Sensitivity (%) ($\Delta R/R_{baseline}$)		-2.299	-0.831	0.098	0.573

Figure Captions

Figure 1. Monochromatic one-way (space-to-ground) transmittance of CO_2 (in blue) and H_2O (in red) at nadir in the 1.58 μm band. The output spectral resolution is $1.4x10^{-3}$ cm^{-1}. 1976 US standard atmosphere is used in the calculation.

Figure 2. Illustration of solar radiation processes as it goes through atmosphere and back to space and test schemes for the radiance sensitivities to CO_2 concentration changes.

Figure 3. The nadir-viewing back-to-space radiance (mW m^{-2}/cm^{-1} sr^{-1}, top panel), the radiance zoom in for 6358-5362 cm^{-1} (middle panel), and the radiance sensitivity to 1 ppmv CO_2 column mixing ratio increase in whole atmosphere (bottom panel) for three spectral resolutions. Solar zenith angle is 30° and surface reflectivity is 0.3.

Figure 4. The back-to-space radiance change for 1% CO_2 concentration increase in the atmospheric boundary layer (0-2 km).

Figure 5. The back-to-space radiance (mW m^{-2}/cm^{-1} sr^{-1}) at 1.58μm band for nadir viewing at 80° solar zenith angle in the upper panel and the radiance change in percentage corresponding to 1% CO_2 concentration increase in the atmospheric boundary layer in the lower panel.

Figure 6. Off-line to on-line radiance ratio sensitivities to 1% CO_2 concentration increase in the atmospheric boundary layer, maritime, rural and urban aerosol extinction, and to cirrus clouds. Off-line frequency is chosen to be 6382.7 cm^{-1}.

Figure 7. The back-to-space radiance change for 1 K error in temperature profile data. The sign of the error for each layer is randomly generated.

Figure 8. The influence of water vapor absorption on the back-to-space radiances.

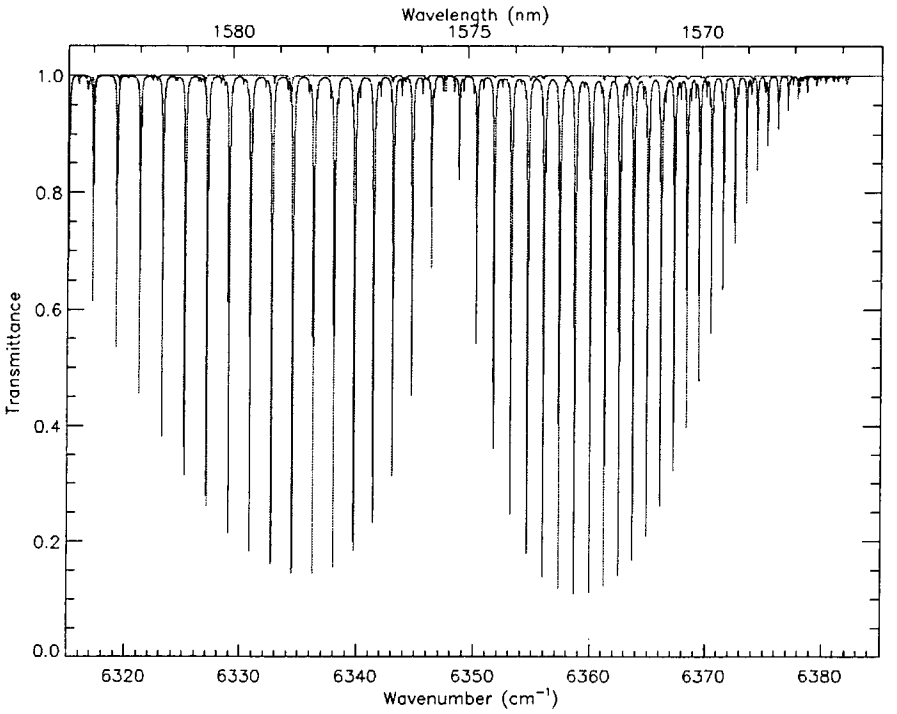

Figure 1. Monochromatic one-way (space-to-ground) transmittance of CO_2 (in blue) and H_2O (in red) at nadir in the 1.58 μm band. The output spectral resolution is 1.4×10^{-3} cm^{-1}. 1976 US standard atmosphere is used in the calculation.

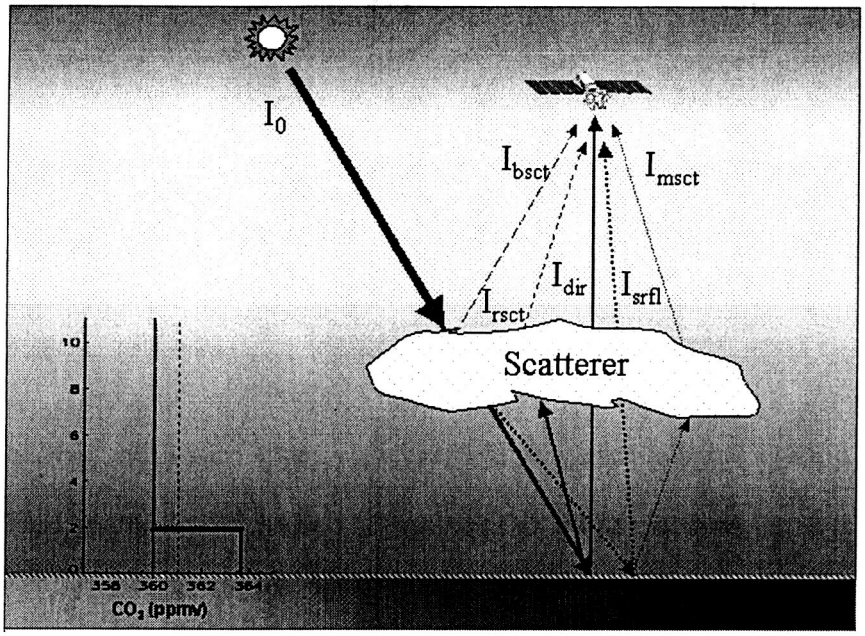

Figure 2. Illustration of solar radiation processes as it goes through atmosphere and back to space and test schemes for the radiance sensitivities to CO_2 concentration changes.

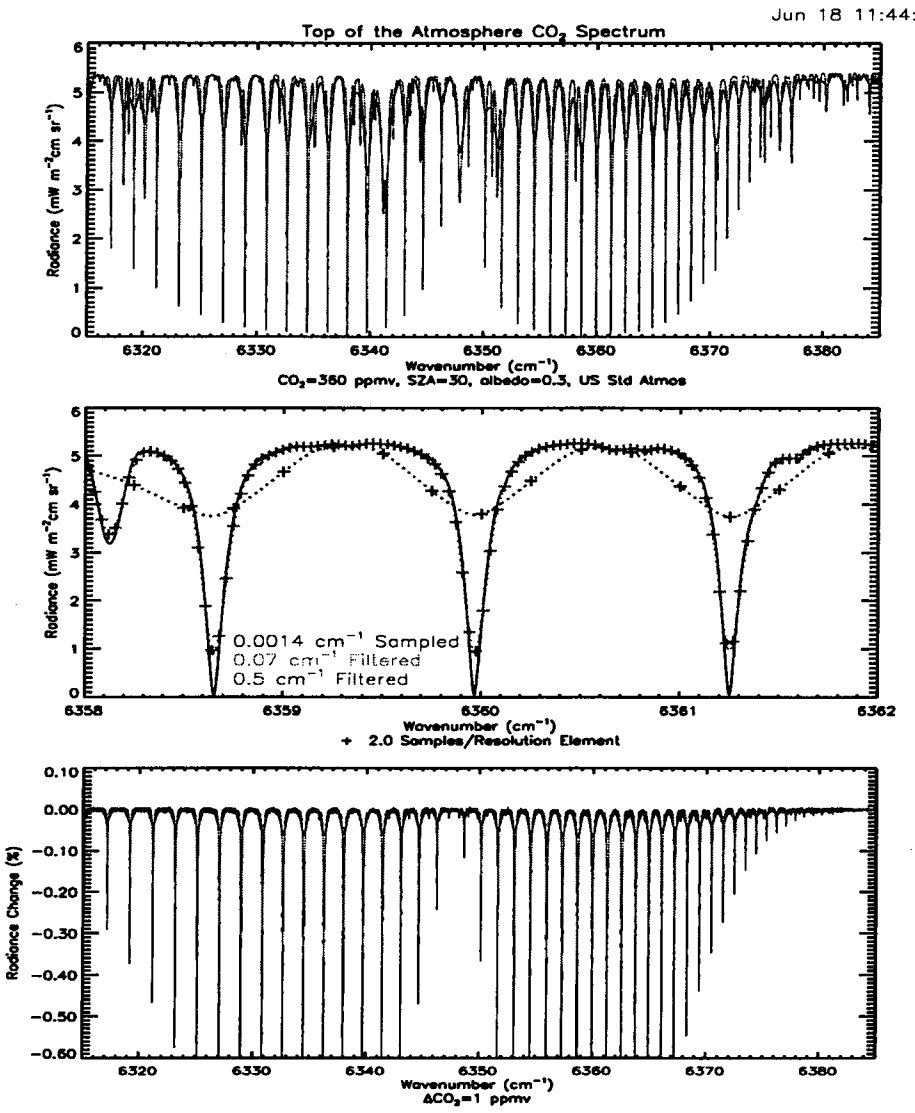

Figure 3. The nadir-viewing back-to-space radiance (mW m^{-2}/cm^{-1} sr^{-1}, top panel), the radiance zoom in for 6358-5362 cm^{-1} (middle panel), and the radiance sensitivity to 1 ppmv CO_2 column mixing ratio increase in whole atmosphere (bottom panel) for three spectral resolutions. Solar zenith angle is 30° and surface reflectivity is 0.3.

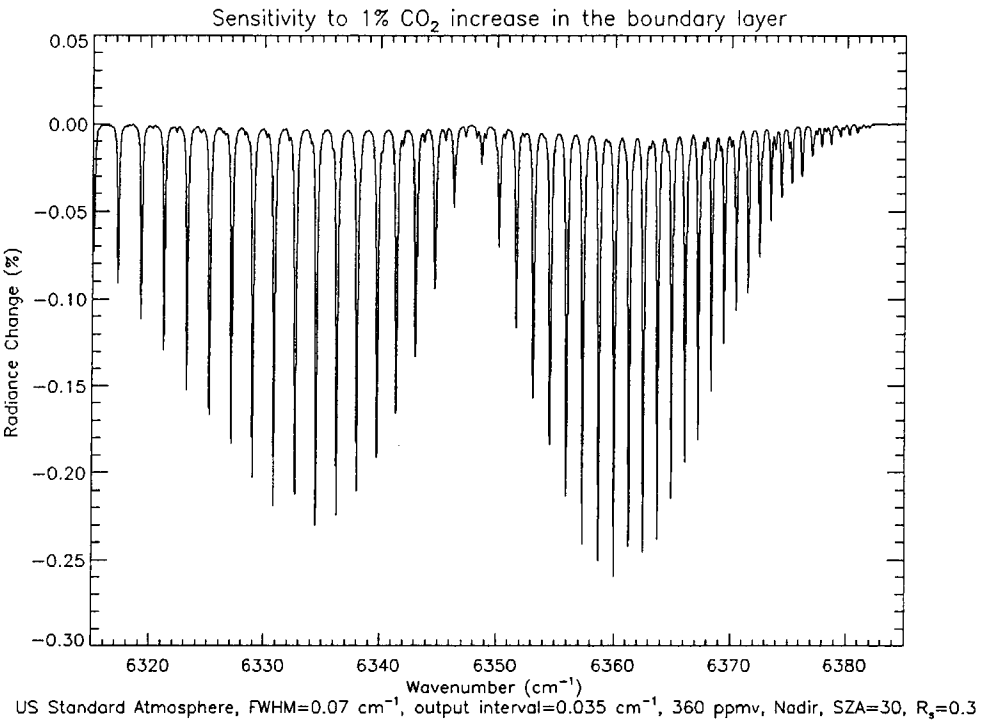

Figure 4. The back-to-space radiance change for 1% CO_2 concentration increase in the atmospheric boundary layer (0-2 km).

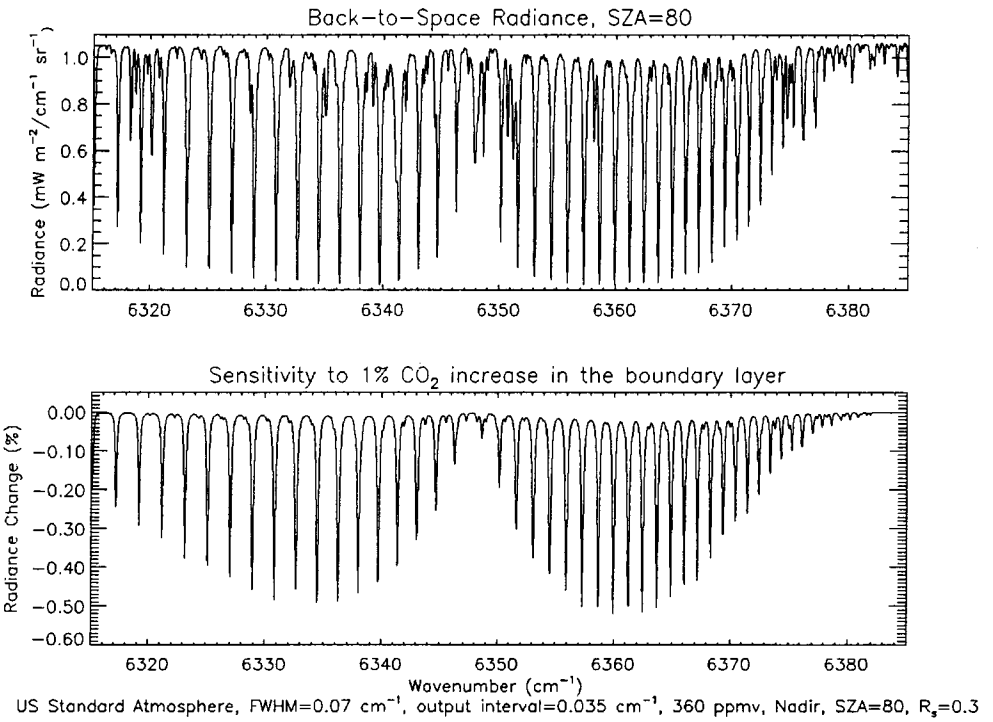

Figure 5. The back-to-space radiance (mW m^{-2} /cm^{-1} sr^{-1}) at 1.58μm band for nadir viewing at 80° solar zenith angle in the upper panel and the radiance change in percentage corresponding to 1% CO_2 concentration increase in the atmospheric boundary layer in the lower panel.

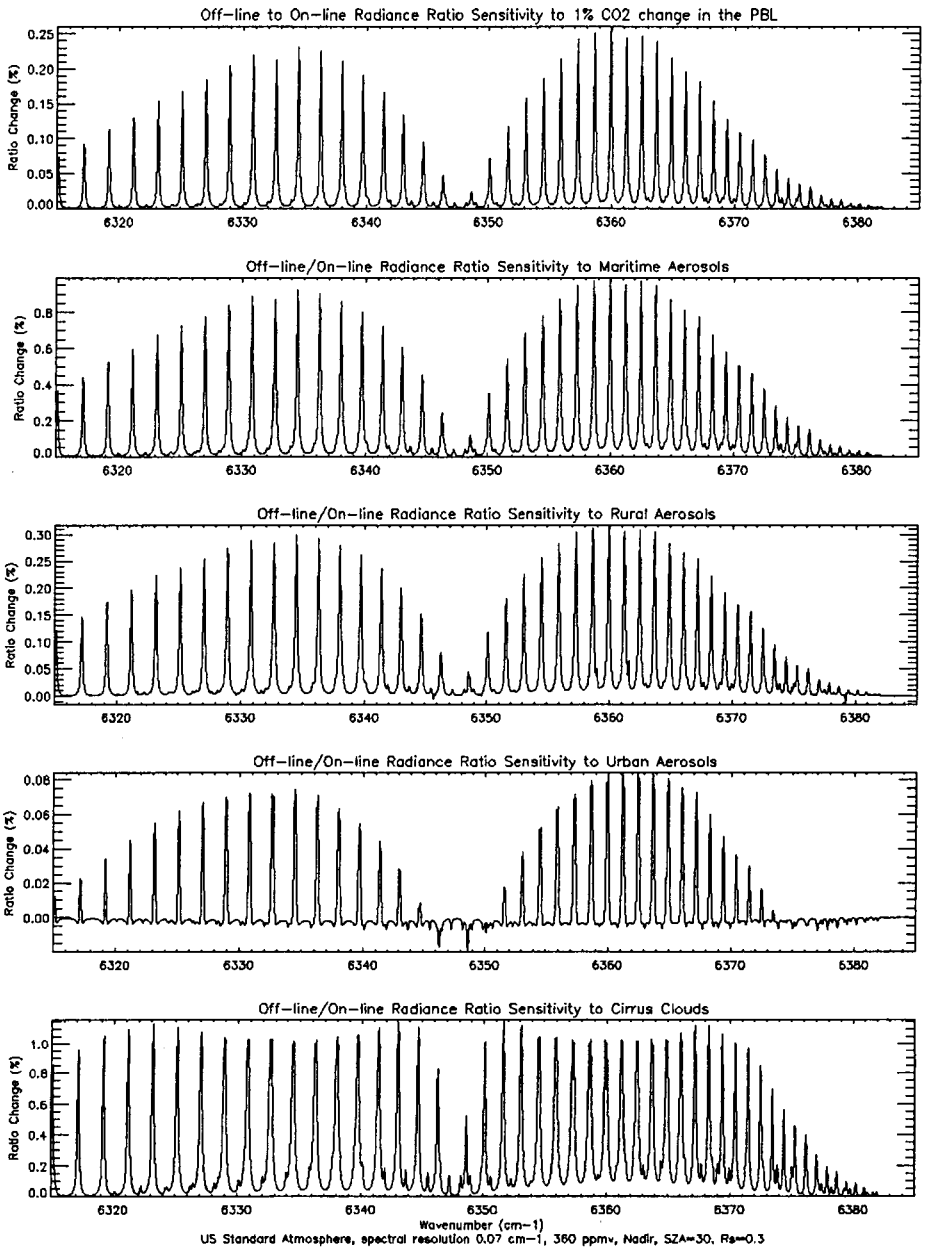

Figure 6. Off-line to on-line radiance ratio sensitivities to 1% CO_2 concentration increase in the atmospheric boundary layer, maritime, rural and urban aerosol extinction, and to cirrus clouds. Off-line frequency is chosen to be 6382.7 cm^{-1}.

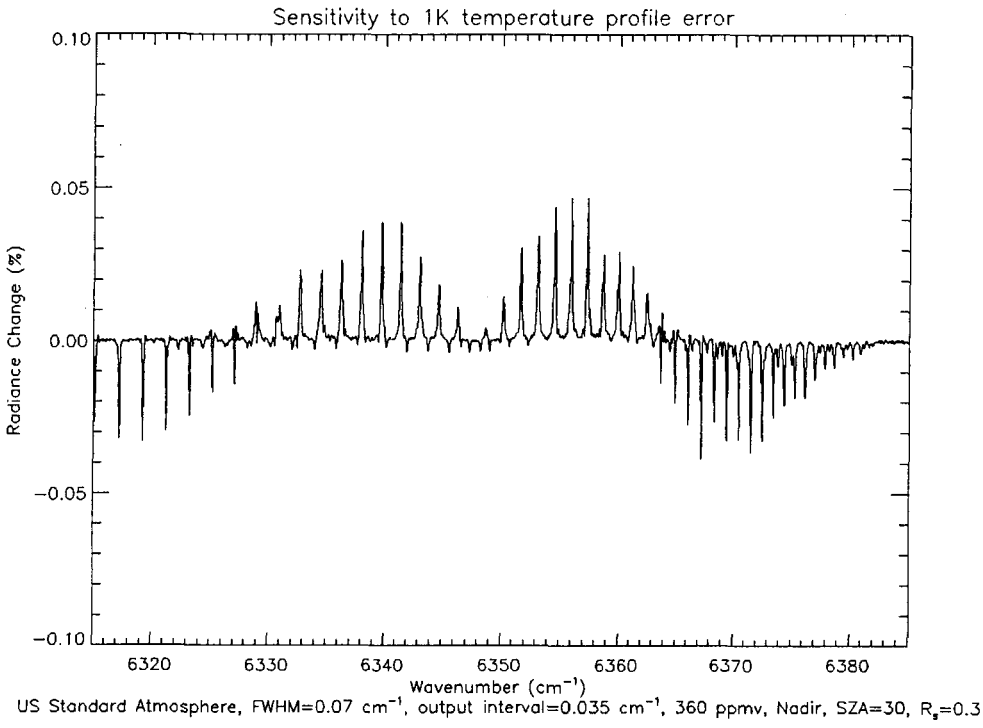

Figure 7. The back-to-space radiance change for 1 K error in temperature profile data. The sign of the error for each layer is randomly generated.

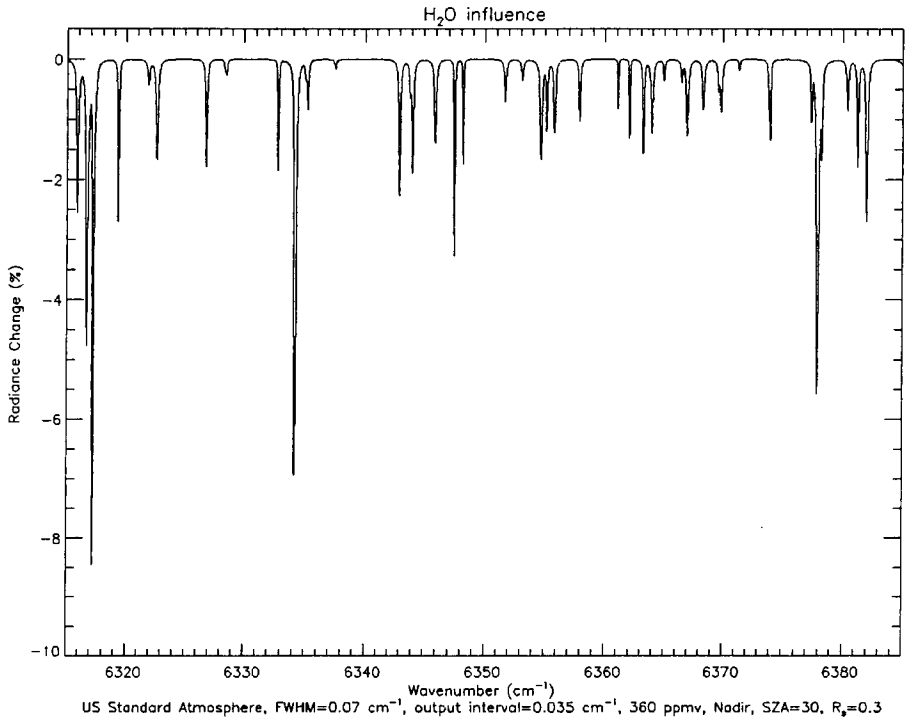

Figure 8. The influence of water vapor absorption on the back-to-space radiances.

Sensitivity Studies for Space-based Measurement of Atmospheric Total Column Carbon Dioxide Using Reflected Sunlight

Popular Summary

A series of sensitivity studies has been carried out to explore the feasibility of space-based carbon dioxide (CO_2) measurements for global and regional carbon cycle studies. The detection method uses absorption of reflected sunlight in the CO_2 band at 1.58 μm. The sensitivities of the detected radiances are calculated using a line-by-line model implemented to include atmospheric scattering in this band. The results indicate that (a) the small (~1%) changes in CO_2 near the Earth's surface are detectable in this CO_2 band provided adequate sensor signal-to-noise ratio and spectral resolution are achievable; (b) the sensitivity to CO_2 change near the surface is not significantly diminished even in the presence of aerosols and/or thin cirrus clouds in the atmosphere; (c) the modification of sunlight path length by scattering of aerosols and cirrus clouds could lead to large systematic errors in the retrieval; therefore, ancillary aerosol/cirrus cloud data are important to reduce retrieval errors; (d) CO_2 retrieval requires good knowledge of the atmospheric temperature profile. We conclude that high precision, space based spectrometric measurements of CO_2 are feasible, but that great care must be taken to avoid potential biases.